Investigating the Role of Classical Cadherin Isoforms in the Control of Collective Cell Migration

INTRODUCTION

Collective cell migration involves the coordinated movement of multiple cells that retain cell-cell contacts while coordinating their actin dynamics and intracellular signalling. For this to occur, cells and their neighbours must coordinate with one another by signalling across cell-cell junctions which requires adhesive interactions between cells. In doing so, a leader cell emerges at the front of the cell group and drives migration of follower cells present in the sheet of collectively moving cells and improves the efficiency of their coordinated migratory behaviour (Mayor & Etienne-Manneville, 2016).

An important type of calcium-dependent adhesion molecule (CAM) involved in these interactions are the cadherins. Cadherins depend on calcium ions and are critical for the formation of adherens junctions which allow cell-cell binding. They are a superfamily classified into primarily four groups: classical, desmosomal, protocadherins, and finally the unconventional group composed of cadherins not classified into either of the three groups. The classical group is composed of E-cadherin (CDH1) normally expressed in epithelial cells, VE-cadherin (CDH5) expressed in endothelial cells, N-cadherin (CDH2) found in neurons, N-cadherin 2 (CDH12), and P-cadherin (CDH3) found in the placenta. In vertebrates there are over 100 different types of cadherins that can be found (Halbleib & Nelson, 2006) but despite the high variety of cadherins, all isoforms share three main components crucial in their function. On the exterior end, a large extracellular domain composed of a single chain of five tandem glycoprotein repeats serves to mediate cell-cell adhesion contact while a smaller highly conserved C-terminal cytoplasmic domain allows association with actin filaments through catenins such as p120-catenin, beta-catenin, and alpha-catenin (Marie et al., 2014). A small transmembrane component is also present that links the extracellular domain to the intracellular cytoplasmic domain. Along with cadherins, other molecules such as integrins which attach the cell cytoskeleton to the extracellular matrix (ECM) and act as traction sites, and protrusions that extend towards the direction of migration which include lamellipodia and filopodia also aid in cell movement. Often, collective cell migration is simplified as a group of cells moving in the same direction. However, this is not the case and it is important to distinguish collective cell migration from a global ordering of cell migration such as long-range chemotaxis. The latter is seen in the polarization of *Dictyostelium discoideum* as well as solitary neutrophils where local chemoattractants act as guidance cues and the overall movement of cells is governed by interaction of each individual cell with the global external stimulus rather than interaction between individuals (Dilla & Sacristan, 2006; Friedl, Locker, Sahai, & Segall, 2012; McCann, Kriebel, Parent, & Losert, 2010).

In this report, we looked at collectively migrating human umbilical vein endothelial cells (HUVEC) to determine how different cadherin isoforms can contribute to cell-cell interactions that affect

collective cell behaviour. Our main analysis focused on how cells coordinated their movements with one another in an unperturbed monolayer when plated at varying densities. We hope that by understanding the mechanisms behind which cells collectively migrate, we can gain further insight into processes such as morphogenesis, wound healing, embryonic development, and cancer invasion (Friedl & Gilmour, 2009) which all fundamentally rely on coordinated cell movement through cell-cell communication across adherens junctions.

MATERIALS AND METHODS

Cell culture. HUVEC cells stably expressing VE, E, and P-cadherin isoforms were grown in 6cm or 10cm plastic dishes and grown in endothelial growth media ("EndoGRO VEGF" Millipore), endothelial basal media supplemented with fetal bovine serum, growth factors and L-glutamine. Hygromycin (50 μg/ml) was added to maintain expression of hTERT-IRES-Hygro, and Puromycin (0.5 μg/ml) was added to maintain expression of CDH5-mCitrine-IRES-Puro, E-cadherin-mCitrine-IRES-Puro, and P-cadherin-mCitrine-IRES-Puro. There were two HT73-E-cadherin-mCitrine cell lines used in different experiments. They are denoted by E-cadherin (old) and E-cadherin (new) with their difference being having unknown VE-cadherin expression remaining and having confirmed depletion of VE-cadherin, respectively. The new E-cadherin cell line was also confirmed to being expressing E-cadherin properly whereas this was not fully confirmed in the old construct.

Cell Fixation and live-cell imaging. Type I Bovine Collagen Solution from Advanced BioMatrix (3mg/ml) was diluted 1:100 with PBS and 100ul of this solution was added to the wells of a glass-bottom 96-well plate. The wells along the perimeter of the plate were unused and coated with 100 ul of diluted collagen solution. The 96-well plate was incubated at 37 ^{o}C overnight or between 16 –24 h after which the collagen solution was aspirated out. Cells were detached from their 6 cm dishes by washing with 5 ml PBS, then 2 ml of trypsin (0.05% Trypsin-EDTA 1X) was added and aspirated out after 30 seconds, and the cells were incubated for 2 min at 37 ^{o}C then resuspended in EGM2. Cells were counted using a hemocytometer and plated at increasing densities of 0.25 x 10^4, 0.5 x 10^4, 1 x 10^4 1.5 x 10^4, and 2 x 10^4 cells per well and incubated at 37 ^{o}C overnight. The wells were then aspirated, and cells were stained with 100 ul Hoechst 33342 nuclear dye diluted 1:50000 in growth media and the plate was incubated for 30 min up to 1 h. The wells were drained and 100 ul of LIS (Live-cell imaging solution: 50 ml ECB, 1% FBS, 2.5 ul of 5 ng/ml bFGF) was added. The plate was sealed with aluminum and incubated for 30 min up to 1 h. Cells were imaged using an automated widefield fluorescence microscope (ImageXpress Micro XLS, Molecular Devices) at 5 min intervals over 25 time points for at total of 2 h using a DAPI-50 filterset and a 4X S Fluor objective.

Cell density conversion. Microscopy images obtained were analyzed by tracking movement of cell nuclei. The number of cells present in the field of view (FOV) at the start of microscopy was converted to a cell density in cells per mm^2. Each image was 2160 by 2160 pixels and each pixel

had a dimension of 1.62 um by 1.62 um (0.00162 mm). The conversion used was x/(2160*2160*0.00162 x 0.00162) to get cells per mm^2 where x is the number of cells present in the microscopy image FOV.

Cell tracking and motility analysis. Custom written MATLAB functions and scripts were used to track cell nuclei. Movement of nuclei was followed through each time frame by using the nearest neighbour method and cells that left the field of view during microscopy received NaN values from that timepoint onwards. Cells entering the FOV during microscopy would be recorded as a new track with data from that time point onwards and NaN values prior to that time frame. Subsequent time points (5 min intervals) were used to calculate single cell velocity by identifying nuclear displacement from one time point to the next and averaging over 25-time points. Unadjusted single cell velocity was calculated by taking all the data and averaging it while adjusted single cell velocity was calculated only from cells that were present within the FOV during the full 2 h of microscopy and ignoring cells that left or entered the FOV during this time. Coordination of cells was quantitatively analysed using the averaged pairwise velocity correlation between an individual cell and its neighbours within a 100 μm radius (Hayer et al., 2016). The front and rear coordination's of a cell were determined by tracking the nuclei of its neighbouring cells within a 60^o sector in front or behind the cell in question and lateral coordination calculated with cells in the remaining 120^o sectors. Splitting of single cell velocity and coordination was done by segregating data into the first half of microscopy and the final half of microscopy.

One-way ANOVA. Statistical tests were conducted on the overall coordination, the front coordination and the rear coordination. Cell densities were split into two bins: 0 – 250 cells per mm^2 and 250 – 500 cells per mm^2 for significance testing between E-cadherin, VE-cadherin, and P-cadherin. The highest density bin 500 – 750 cells per mm^2 was not tested as there was variability in cell density and not all of the cadherin-expressing cell lines were plated to densities reaching this upper range (E-cadherin).

One-way ANOVA was used as only one factor was tested: cadherin isoforms. The dependent variable was the coordination scores. The three assumptions made for one-way ANOVA are as follows: the dependent variable (Coordination Score) is normally distributed, there is homogeneity of variance such that population variances (distribution or spread of scores around the mean) of all three cadherins (VE, E, and P) tested are equal, and finally the coordination values of each cadherin are independent of each other. The open-source programming language R was used to run one-way ANOVA and post-hoc tests. The null hypothesis (H_0) was that there is no difference in coordination scores between VE-, E-, and P-cadherins. The alternative hypothesis (H_1) was that there is at least one difference coordination scores between the three cadherin isoforms. The confidence interval was set at 95% for ANOVA and p-values ≤ 0.05 indicated a statistically significant difference in coordination scores and a post hoc test was used to confirm which two cadherin isoforms displayed the difference by setting $P \leq 0.05$.

Post-hoc analysis.

Tukey's honestly significant difference (HSD) post-hoc test was used on the 0 – 250 cells per mm^2 group since the requirements of independence of coordination scores among cadherin

isoforms, a normal distribution, homogeneity of variance, and having a balanced design were met (Minitab, 2015). Tukey was used over Scheffé post-hoc test as Tukey is less conservative, allowing differences to be detected more easily (Lund & Lund, 2013).

The Games-Howell Test was used on the 250 – 500 cells per mm^2 group since this group did not have a balanced design. The Games-Howell Test is more flexible than Tukey as unbalanced designs are acceptable, and the assumptions of homogeneity of variance and normality are not required.

Immunofluorescence. 20 ml of fixation solution (5 ml of 16% formaldehyde solution, 0.2 ml of 1M HEPES pH 7.4, 14.8 ml PBS) was created and 50 ul was added to each well containing 50 ul of growth media already. Permeabilization or blocking step was done by adding 35 ul ASBB (For 20 ml: 100 ul blocking/antibody dilution buffer 0.1% Triton X-100, 2 ml Fetal Bovine Serum, 2 ml BSA, 100 ul NaN_3, 15.8 ml PBS) and the plate was incubated at room temperature for 30 min. Immunostaining was done by adding 35 ul of primary antibody diluted in ASBB (1:400 or 1.25 ul AB with 500 ul ASBB) and incubated for 2 h at RT. After washing with PBS, 35 ul secondary antibody diluted 1:1000 in ASBB was added and washed with PBS prior to imaging. Full protocol available upon request.

Immunofluorescence images were analyzed in FIJI by setting the Brightness and Contrast to the same level for both the E-cadherin and VE-Cadherin images using the Set command to allow for an accurate comparison of intensity within cadherin junctions. The Texas-Red channel was used in the analysis.

All code used in this report to analyze data such as coordination and single cell velocity is available upon request.

RESULTS

To investigate how different cadherin isoforms affect collective cell migration, we functionally replaced endogenously expressed VE-cadherin in HUVEC by transducing them with lentivirus encoding E-cadherin and P-cadherin. Localization of classical cadherins at the cell surface is stabilized by association with p120-catenin. In the absence of p120-catenin, cadherins get rapidly internalized (Xiao, Oas, Chiasson, & Kowalczyk, 2007). When exogenous cadherins are (over)expressed in cells, p120-catenin becomes limiting and the exogenously expressed cadherin functionally replaces the endogenous cadherin (Hayer et al., 2016; Xiao et al., 2007).

E-cadherin cells (old construct) have higher single cell velocity than VE-cadherin cells across all cell densities

To gain insight into how cells collectively migrate and coordinate their movement relative to one another, a first step would be to check their single cell velocity as a control. From time-lapse microscopy imaging, we observed that from the lowest to highest cell densities plated (~100 – 750 cells per mm^2), E-cadherin cells appeared to have a higher single cell velocity than VE-cadherin cells (Fig. 1a). E-cadherin cell velocity appear to remain relatively consistent at ~23 um per hour across different densities with a large dip at 200 cells per mm^2 but this was also seen in

VE-cadherin cells and may be due to external factors rather than an inherent property of the cells. On the other hand, VE-cadherin cells display a peak velocity between 19 – 20 um per hour at a density of ~400 cells per mm^2 and velocity begins to fall when approaching higher densities. When adjusting the single cell velocity by only calculating single cell velocity from cells that remained within the field of view of the microscope during the entire imaging period, we found that the average speed of cells decreased but the general trend remained consistent (Figure S1).

E-cadherin (old construct) have higher coordination than VE-cadherin at low cell densities but at peak coordination VE-cadherin cells are more coordinated

When looking at the coordination (Fig. 1b), cells expressing E-cadherin appeared to have higher coordination than VE-cadherin at low cell densities such as at 100 and 200 cells per mm^2 and as cell densities increase, coordination peaks between 400 – 450 cells per mm^2 for both VE-cadherin and E-cadherin cells at 0.1 and ~0.85 respectively. Higher densities of cells show a more ambiguous result for coordination difference with both E-cadherin and VE-cadherin displaying a similar trend as the cells become less coordinated with each other. Since cells may have needed time to adjust to the conditions under the microscope we decided to take this into account by splitting the calculation of coordination into the first hour of imaging and the second hour of imaging (Fig. 1c). Our results argue that cells do in fact require some time to stabilize and readjust to the new conditions during imaging as we see that in the first hour of microscopy both E-cadherin and VE-cadherin cells at low densities had a more variable average coordination. In the second hour of imaging, these lower densities had coordination values nearer one another demonstrating that cells have now become more accustomed to the environment. Furthermore, the difference in peak coordination values for E-cadherin and VE-cadherin at ~450 cells per mm^2 became more pronounced as VE-cadherin coordination increased. We then calculated coordination by segregating a cell's neighbours into a 60^o sector in front of the cell, a 60^o sector behind and a 120^o sector on the sides of the cell and used to calculate the front, lateral and rear coordination respectively. For front coordination (Fig. 1d) we noticed that coordination values across all cell densities were shifted up and were much higher with peak coordination reaching 0.16 for VE-cadherin and 0.13 for E-cadherin. The general trend of VE-cadherin having lower coordination than E-cadherin at low cell densities and higher peak coordination at 400 cells per mm^2 was not only observed but became more pronounced. In the lateral coordination, there was little to no distinction between the two cadherin cell types (Fig. 1e). The coordination peaked at 0.07 but this time at ~550 cells per mm^2. In the rear (Fig. 1f), results were very similar to front coordination as expected since each follower cell itself is a leader cell with follower cells so coordination in the front and back should be consistent. Further analysis was done by splitting each of the front, lateral, and rear coordination into the first half of imaging and the second half (Fig. 1g). Our results demonstrate that in the second half of microscopy, peak coordination values increased for the front and rear coordination for both VE- and E-cadherin cells but remain relatively the same for the lateral coordination.

a

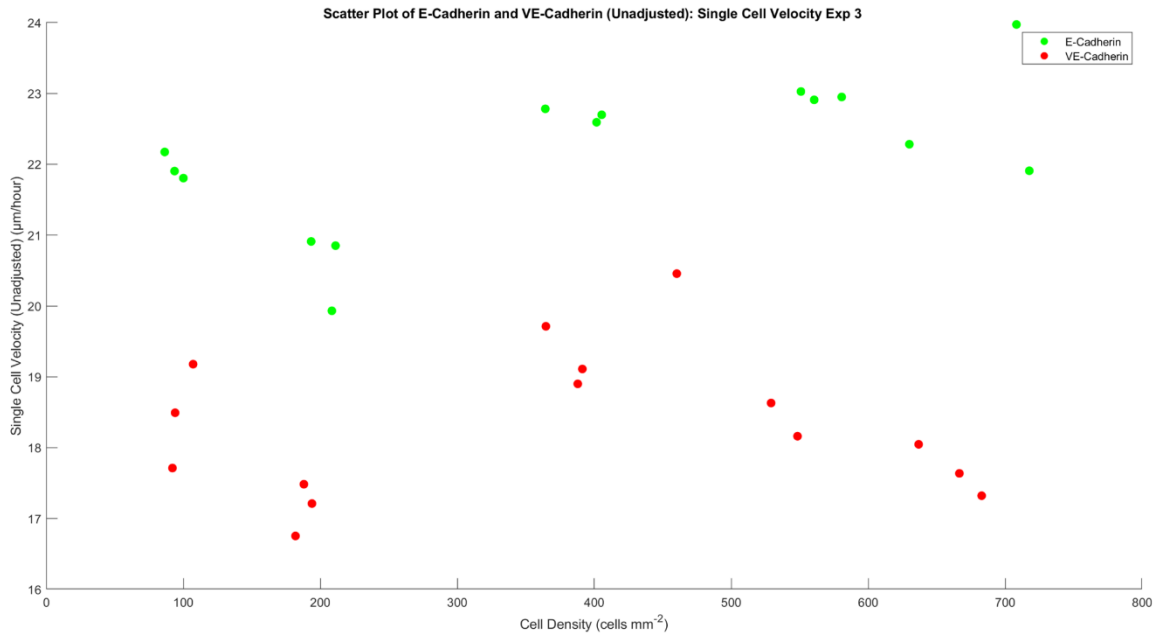
Scatter Plot of E-Cadherin and VE-Cadherin (Unadjusted): Single Cell Velocity Exp 3
E-Cadherin
VE-Cadherin
Single Cell Velocity (Unadjusted) (μm/hour)
Cell Density (cells mm^{-2})
24
23
22
21
20
19
18
17
16
0
100
200
300
400
500
600
700
800

b

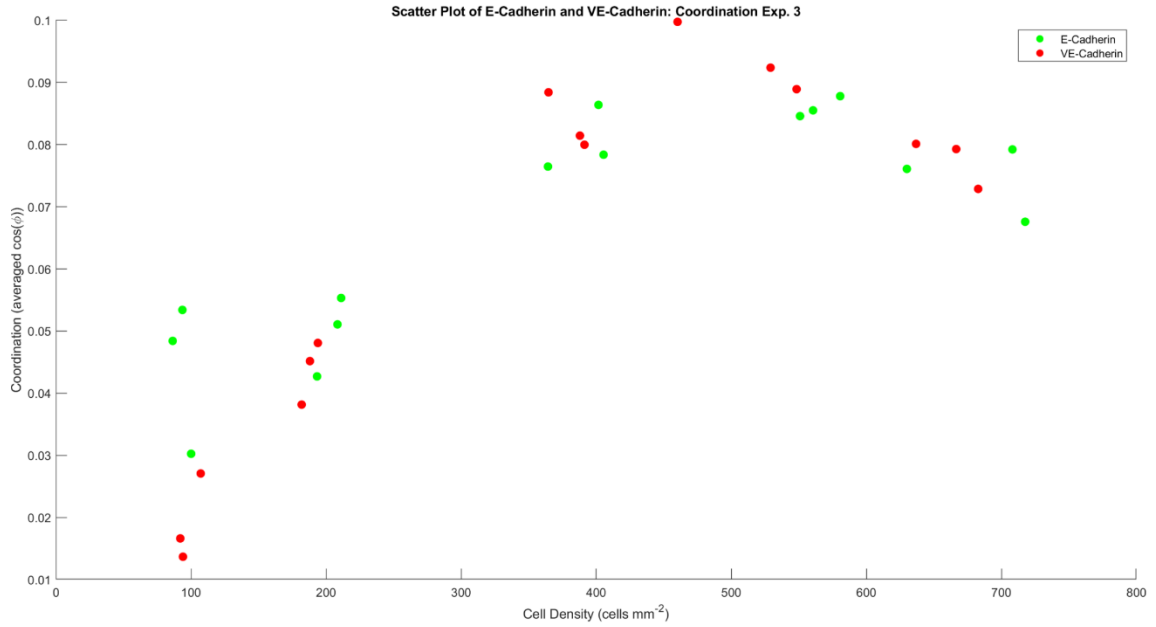
Scatter Plot of E-Cadherin and VE-Cadherin: Coordination Exp. 3
E-Cadherin
VE-Cadherin
Coordination (averaged cos(ϕ))
Cell Density (cells mm^{-2})
0.1
0.09
0.08
0.07
0.06
0.05
0.04
0.03
0.02
0.01
0
100
200
300
400
500
600
700
800

c

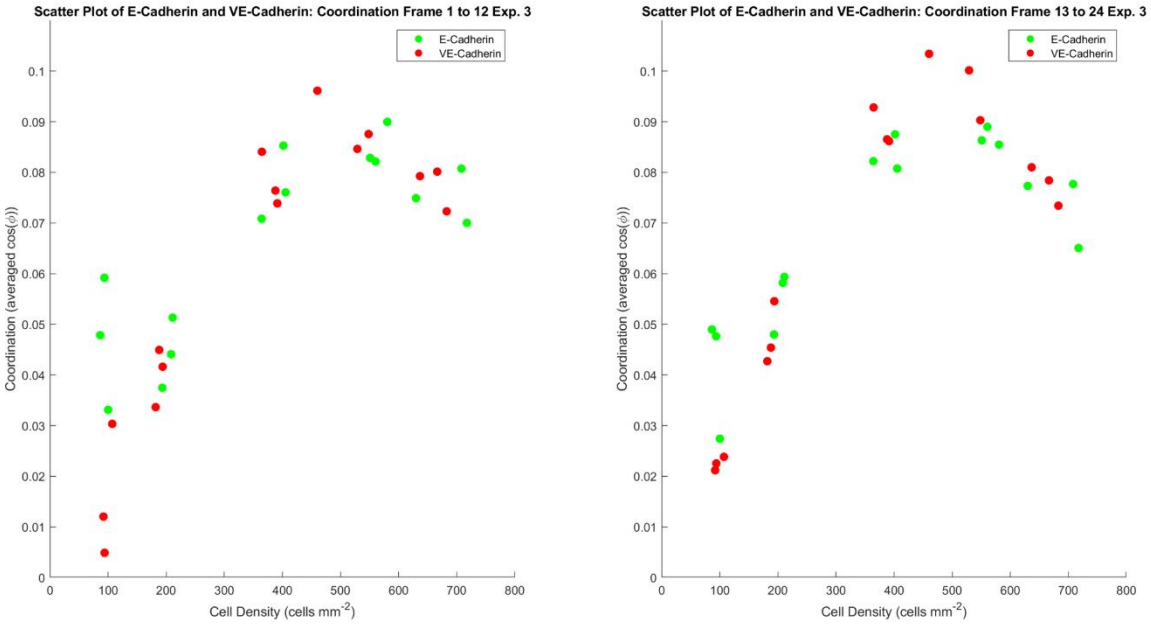
Scatter Plot of E-Cadherin and VE-Cadherin: Coordination Frame 1 to 12 Exp. 3
E-Cadherin
VE-Cadherin
Coordination (averaged cos(ϕ))
Cell Density (cells mm-2)
Scatter Plot of E-Cadherin and VE-Cadherin: Coordination Frame 13 to 24 Exp. 3
E-Cadherin
VE-Cadherin
Coordination (averaged cos(ϕ))
Cell Density (cells mm-2)

d

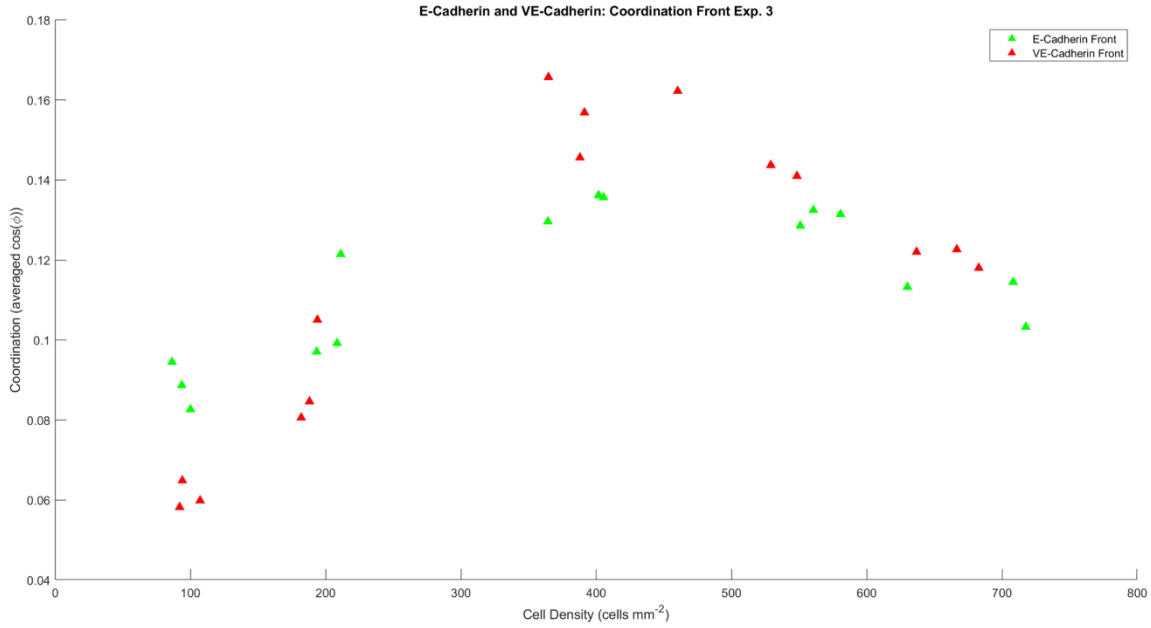
E-Cadherin and VE-Cadherin: Coordination Front Exp. 3
E-Cadherin Front
VE-Cadherin Front
Coordination (averaged cos(ϕ))
Cell Density (cells mm-2)

e

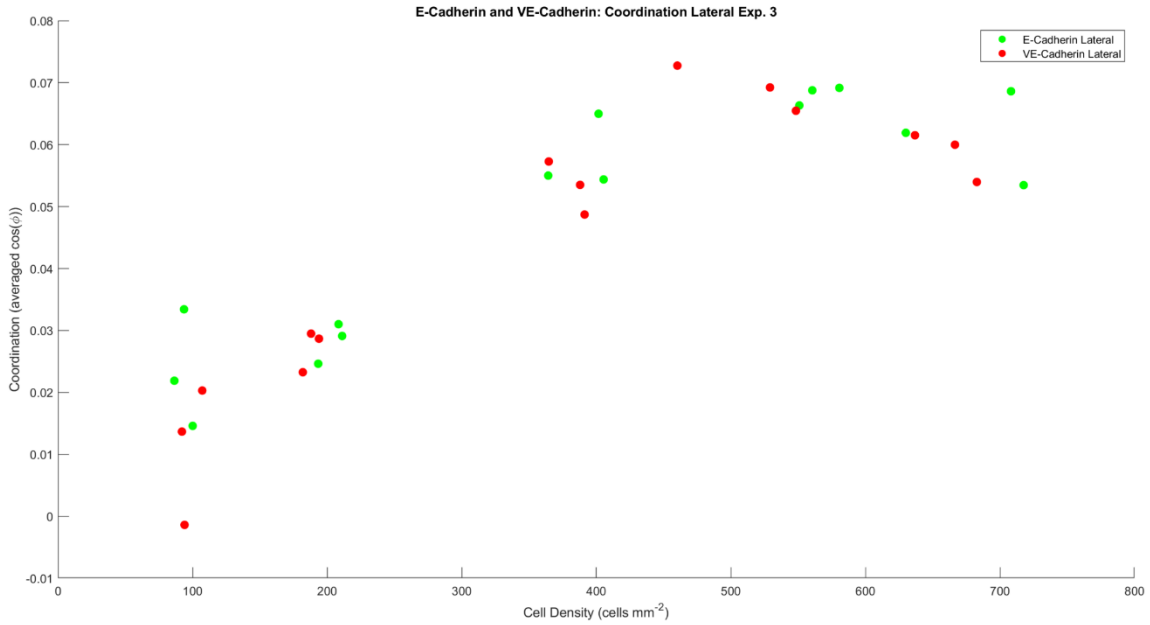
E-Cadherin and VE-Cadherin: Coordination Lateral Exp. 3
E-Cadherin Lateral
VE-Cadherin Lateral
Coordination (averaged cos(φ))
Cell Density (cells mm-2)
0.08
0.07
0.06
0.05
0.04
0.03
0.02
0.01
0
-0.01
0
100
200
300
400
500
600
700
800

f

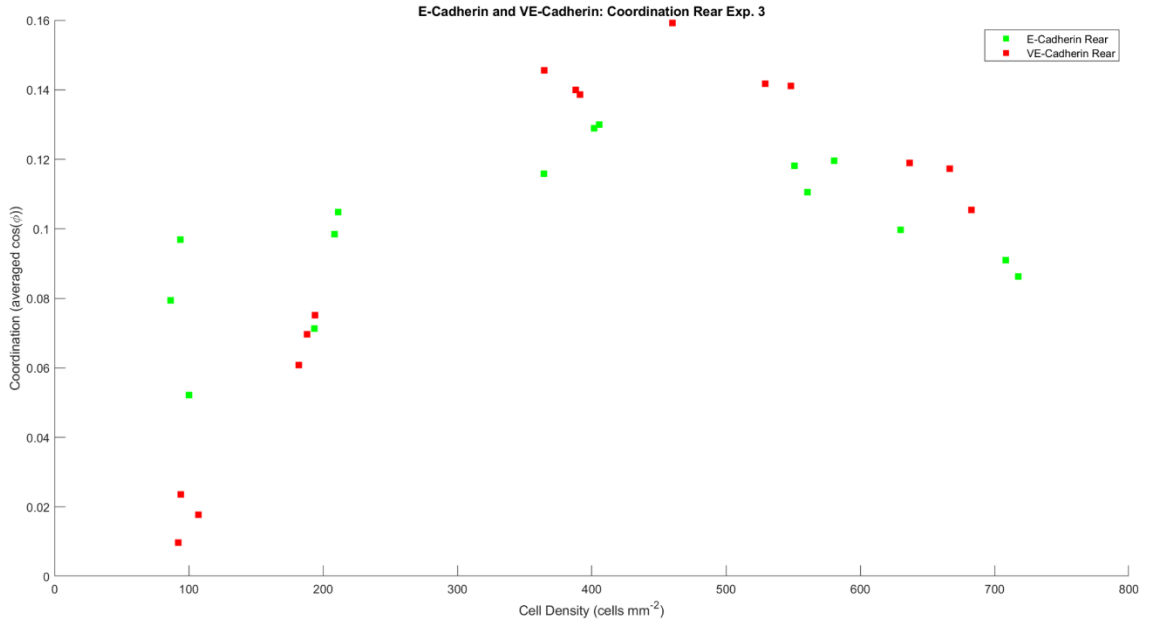
E-Cadherin and VE-Cadherin: Coordination Rear Exp. 3
E-Cadherin Rear
VE-Cadherin Rear
Coordination (averaged cos(φ))
Cell Density (cells mm-2)
0.16
0.14
0.12
0.1
0.08
0.06
0.04
0.02
0
0
100
200
300
400
500
600
700
800

g

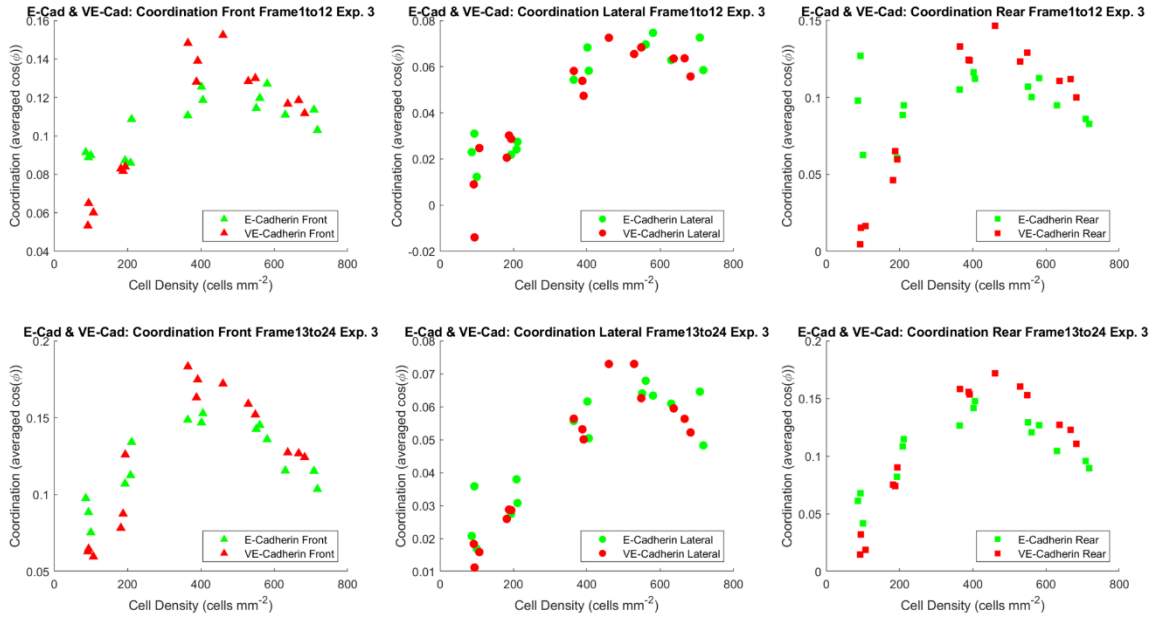

Figure 1 Cell motility analysis of E-cadherin (old construct) and VE-cadherin. Each individual data point is the average value obtained from the cells within a well and all data was obtained from a single experiment. **(a)** HUVECs stained with nuclear dye (Hoechst) were imaged for 2 h at 5 min intervals and MATLAB scripts were performed to calculate single cell velocity in um per hour as a function of cell density in cells per mm^2 within unperturbed monolayers. The E-cadherin construct showed a higher overall velocity across all cell densities compared to the VE-cadherin cells. **(b)** Coordination of cells as a function cell density. **(c)** Coordination of cells split into two sections with the left graph representing coordination of HUVECs during the first hour of microscopy and the right graph measuring coordination during the second hour of microscopy with both being functions of cell density. **(d)** The front coordination of cells as a function of cell density. The front coordination is determined from neighbours within a 60° sector in front of the cell of interest. **(e)** The lateral coordination of cells as a function of cell density. The lateral coordination is calculated from the neighbours within a 120° sector on both sides of a cell. **(f)** The rear coordination of cells as a function of cell density. Rear coordination is calculated from neighbours within a 60° sector behind the cell of interest.

Immunofluorescence analysis shows little VE-cadherin expression left in the E-cadherin (old) construct.

E-cadherin cells (old) were HUVEC expressing E-cadherin but of unknown levels as expression of VE-cadherin leftover was undetermined. It is known that since p120-catenin is a limiting factor for cadherin surface expression, the more of one type of cadherin being expressed such as E-cadherin, the greater the chance of flushing out the other cadherin type, in this case VE-cadherin (Xiao et al., 2007). After fixing cells and immunstaining with primary and secondary antibody diluted in ASBB, images were taken of the E-cadherin (old) and VE-cadherin cells (Fig. 2) with the Texas-red channel. For the E-cadherin cells (Fig. 2a), intensity around the junctional areas of cells was negligible and most of the regions of high intensity correspond to nuclear

regions of the cell, i.e. unspecific background signal of the antibody. For the VE-cadherin cells, high intensity regions were seen in cell-cell juntional regions as expected. Together, these data argue that the E-cadherin (old) should have sufficient downregulation of VE-cadherin but we still did not fully trust the E-cadherin (old) construct since we were not entirely convinced that they were truly expressing E-cadherin in their adheren junctions. To account for this, we created a new E-cadherin cell line for further experiments.

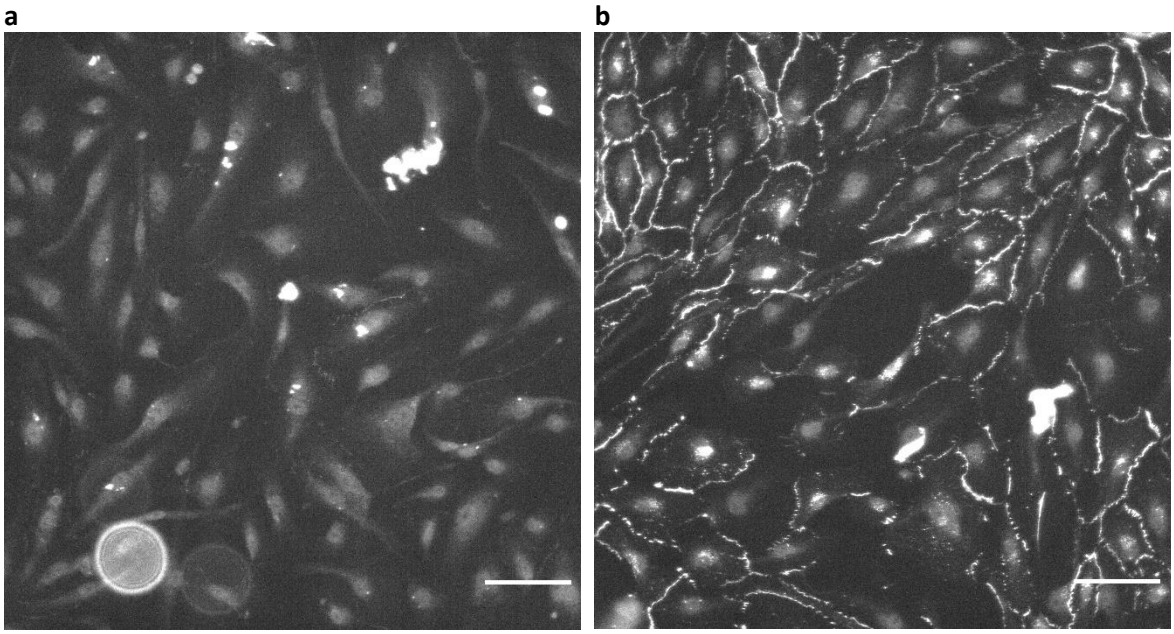

Figure 2 Immunofluoresence analysis of the E-cadherin (old) and VE-cadherin expression levels in junctional regions of HUVECs. Cells were fixed and stained with primary and secondary antibody diluted in ASBB. Images were visualized with the Texas-Red channel. **(a)** E-cadherin (old) cells and **(b)** VE-cadherin cells. Scale Bar, 100 um.

P-cadherin cells show higher single cell velocity than E-cadherin (new) and VE-cadherin

We introduced two new cell types: a P-cadherin cell line and a new E-cadherin cell line where E-cadherin was fully expressed in junctional areas and VE-cadherin was assumed to be fully downregulated. Before analysis of of coordination of cells, we first looked at single cell velocity as a control to make sure cells were actually moving (Fig. 3a). We noticed a large difference in speed of cells of P-cadherin compared to E-cadherin (new) and VE-cadherin. P-cadherin cells were moving extremely fast at close to 30 um per hour and 24 um per hour at a density greater than 500 cells per mm^2, much higher than the average speed of enothelial cells which were reported to be close to 20 um per hour (Engle, K. M.; Mei, T-S.; Wasa, M.; Yu, 2008). A clear segregation of speed of cells is seen with the P-cadherin being the fastest, E-cadherin being moderately fast at 21 um per hour and VE-cadherin being the slowest of the three at 18 um per hour. We then split the data into the first hour of imaging and second hour of imaging and found the difference in single cell velocity to be even greater with the P-cadherin cells peaking

at 32 um per hour in the second hour of microscopy (Fig. 3a). Furthermore, there was an even clearer distinction between the speed of the three cell lines. When adjusting for single cell velocity by only calculating from cells that remained within the field of view of the microscope during the entire imaging period of two hours, we found that single cell velocity remained relatively consistent with our results (Fig. S2a,b).

a

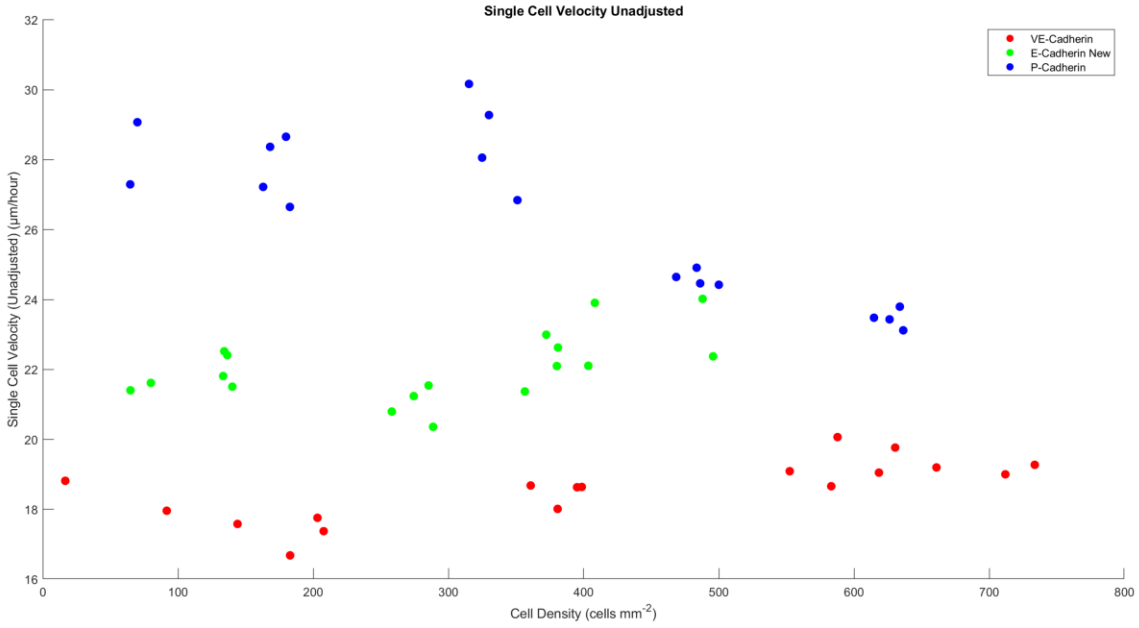

b

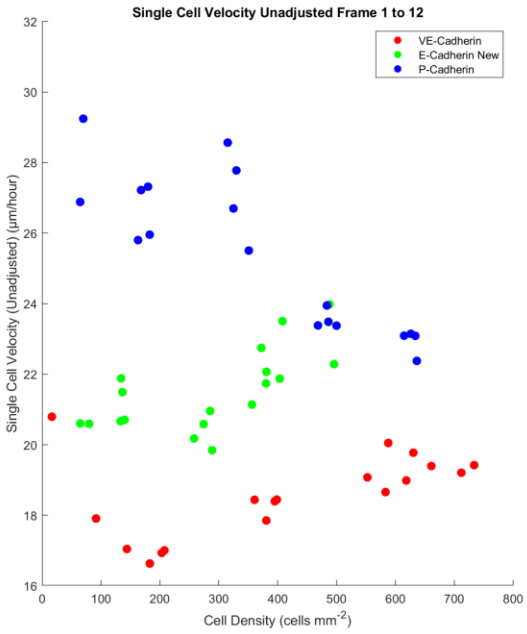

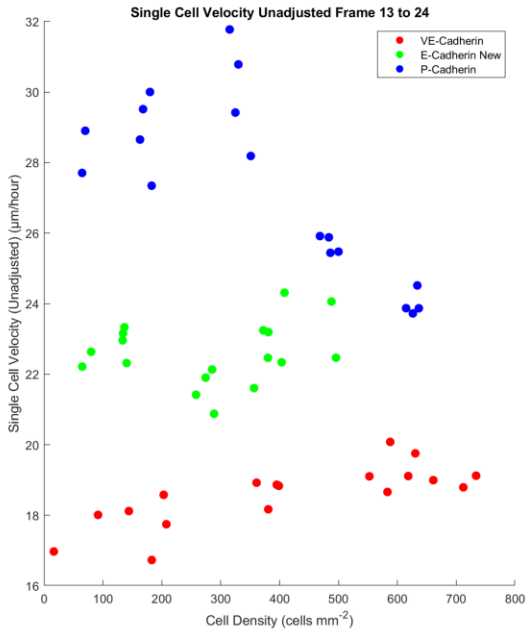

Figure 3. Single cell velocity analysis of VE-cadherin, E-cadherin(new) and P-cadherin-expressing HUVEC in an unperturbed monolayer. Each data point corresponds to the averaged velocity of cells in an entire well of a 96-well plate and corresponds to one experiment. **(a)** The single cell velocity of cells over 2 hours of imaging and **(b)** The single cell velocity of cells split between the first hour of microscopy imaging (left) and the second hour of imaging (right) as a function of cell density.

There is a significant difference in average coordination between P-cadherin and VE-cadherin at low cell densities.

When looking at coordination of cells, there was not as clear of a discrimination between cells aside from the P-cadherin seeming to have a rapid decrease in coordination at cell densities higher than 400 cells per mm^2 (Fig. 4a). We also split the coordination results into the first hour of microscopy and the second half of microscopy and found that results were generally similar (Fig. S3). We decided to test for a significant difference between the coordination of the three cell lines with one-way ANOVA. Our null hypothesis was that there was no significance between E-, VE-, and P-cadherin coordination values. To test coordination, we binned the cell densities into 2 groups representing 0 – 250 cells per mm^2 and 250 – 500 cells per mm^2 with the 500 – 750 cells per mm^2 group untested since E-cadherin cell densities did not reach this high. For the 0 – 250 cells per mm^2 group, ANOVA gave a p-value of 0.0158, less than the standard 0.05 and we concluded that there was a significant difference between VE-, E-, and P-cadherin coordination by rejecting our null hypothesis (Appendix 1). To test which two cadherin cell lines were significantly different, we used Tukey's Honestly significant difference Test (HSD). By setting the confidence level at 95%, we found that there was a significant difference ($p = 0.012$) between P- cadherin and VE-cadherin and no difference between E-VE and P-E-cadherin coordination with p-values of 0.260 and 0.243 respectively. For the 250 – 500 cells per mm^2, ANOVA showed that there was no significant difference between the coordination of the three cell lines ($p = 0.115$) (Appendix 2).

VE-cadherin, E-cadherin (new) and P-cadherin have front coordination values significantly different from each other withinin both ranges of 0 – 250 cells per mm^2 and 250 – 500 cells per mm^2

The front coordination was calculated by taking neighbours located within a 60^o sector in front of the cell of interest and results were quite different from the overall coordination values. In the front coordination (Fig. 4b), even at low cell densities between 0 – 250 cells per mm^2 we see a clear distinction between the P-cadherin coordination and the VE- and E-cadherin coordinations. Furthermore, the P-cadherin coordination became much more pronounced reaching a peak of 0.23 whereas the VE-cadherin and E-cadherin front coordination values only peaked at 0.14 and 0.12 respectively. To confirm this, one-way ANOVA was performed on the front coordination to test for significance. From our ANOVA analysis (Appendix 3) on the binned group composed of wells with densities between 0 – 250 cells per mm^2, we discovered there was high significance ($p = 1.07 \times 10^{-5}$) and Tukey HSD showed significance in all three comparisons, E-VE, P-VE, and P-E with p-values of 0.039, 0.000, and 0.001 respectively. Coordination peaked for P-cadherin at ~350 cells per mm^2, while E-cadherin and P-cadherin both had peak coordination when plated at 400 cells per mm^2. We performed ANOVA on wells within the 250 – 500 cells per mm^2 range (Appendix 4) and found that there was a significant

difference between the coordination scores of all three cadherin isoforms ($p = 2.02 \times 10^{-9}$). Further analysis with the Games-Howell test showed that all 3 comparison groups were significantly different from each other. Since in the overall coordination, at peak coordination P-cadherin was not significantly different from the E-, and VE-cadherin we hypothesized that the lateral coordination must be the main reason masking this difference. The rear coordination was calculated by taking neighbours within a 60^o sector behind the cell of interest and results showed a similar trend to front coordination results aside from coordination values being slightly lower (Fig. 4d). The front, lateral and rear coordinations were split into the first hour of microscopy and second hour of microscopy to get a clearer representation of coordinated movements between cells (Fig. 4e). The axes were adjusted so that the limits were along the same range (Fig. 4f) to show the difference between coordinated movements in the front, lateral, and rear of cells with respect to one another.

Lateral coordination is lower for P-cadherin at densities above 300 cells per mm^2 compared to E-cadherin (new) and VE-cadherin and rapidly decreases at higher cell densities

The lateral coordination was calculated from neighbours within the regions between the front and rear (Fig. 4c). At low cell densities between 0 – 250 cells per mm^2 neither of the three cadherins seemed to be discernable from each other in terms of lateral coordination. We tested this with ANOVA and confirmed that there was no significance between the three cadherins ($p = 0.501$) (Appendix 5). However, between 250 – 500 cells per mm^2 results demonstrated that P-cadherin cells were less coordinated than both E-cadherin and VE-cadherin cells which had similar lateral coordination trends (Appendix 6). ANOVA analysis argued that there was a significant difference between the three cadherins ($p = 0.0002$) and the Games-Howell post hoc test suggested the differences to be between P-E and VE-P cadherins ($p = 0.0004$ and $p = 0.003$ respectively). Furthermore, P-cadherin cells decreased in lateral coordination much more rapidly as cell densities increased above 500 cells per mm^2 while E- and VE-cadherin cells plateaued at higher densities creating an even larger difference in how these cadherin types coordinate their movements laterally relative to one another.

a

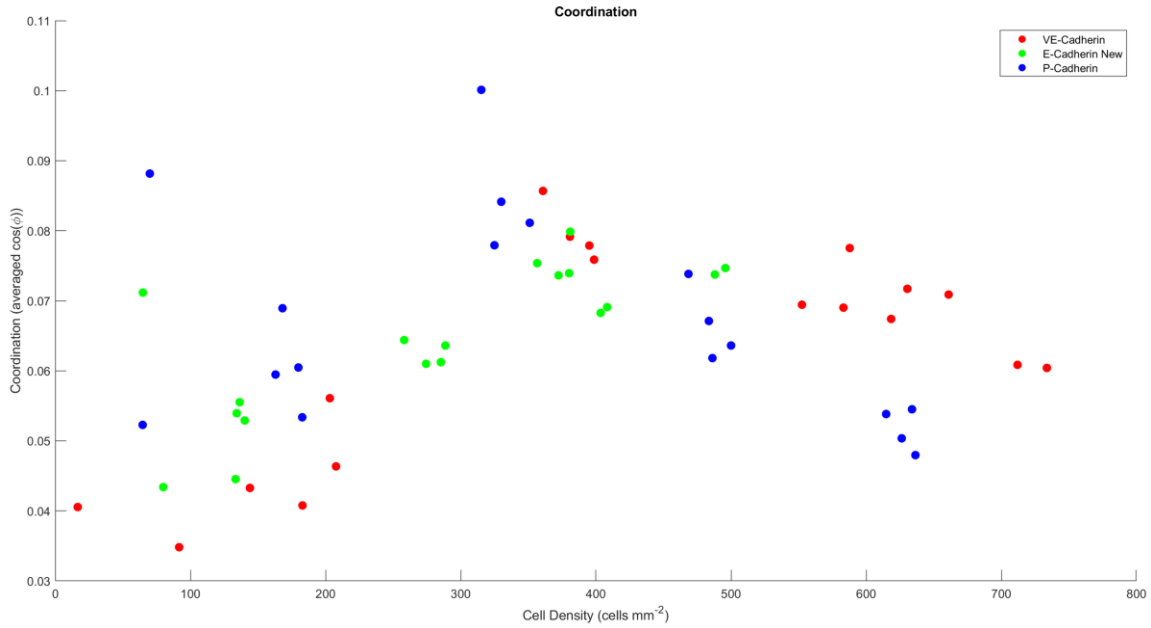
Coordination
VE-Cadherin
E-Cadherin New
P-Cadherin
Coordination (averaged cos(ϕ))
Cell Density (cells mm^{-2})
0.11
0.1
0.09
0.08
0.07
0.06
0.05
0.04
0.03
0
100
200
300
400
500
600
700
800

b

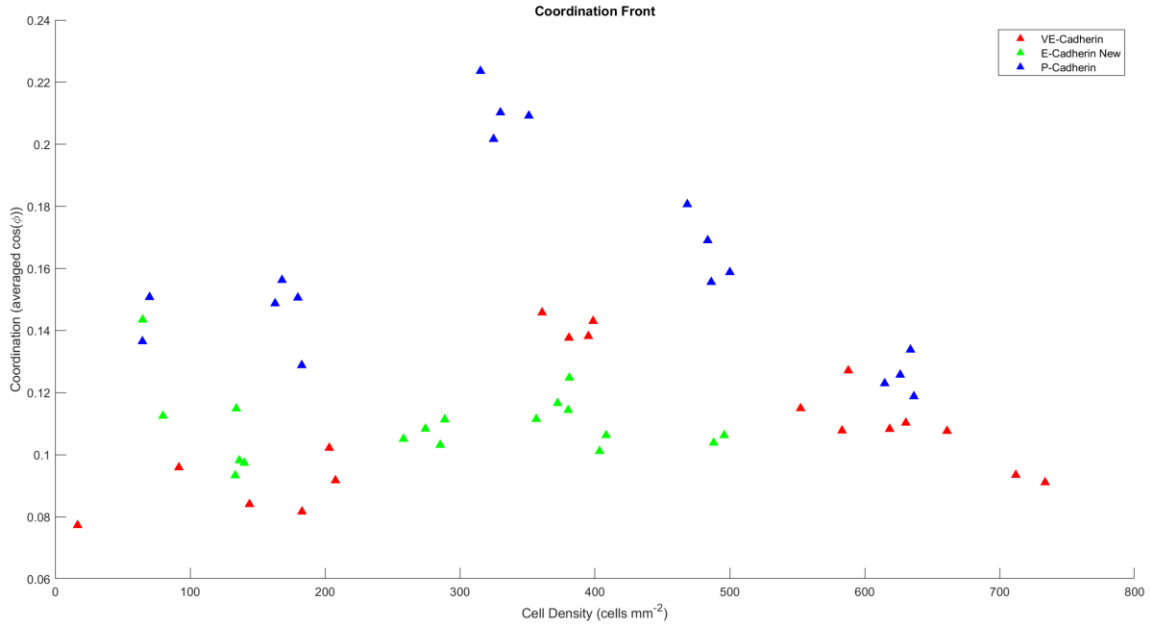
Coordination Front
VE-Cadherin
E-Cadherin New
P-Cadherin
Coordination (averaged cos(ϕ))
Cell Density (cells mm^{-2})
0.24
0.22
0.2
0.18
0.16
0.14
0.12
0.1
0.08
0.06
0
100
200
300
400
500
600
700
800

c

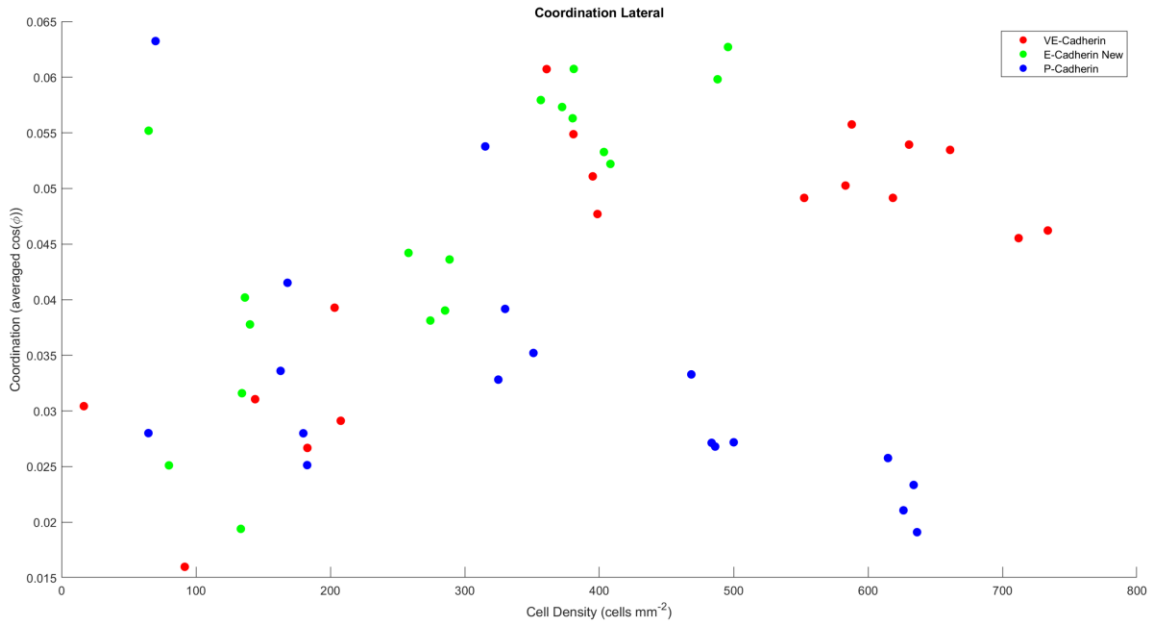
Coordination Lateral
VE-Cadherin
E-Cadherin New
P-Cadherin
Coordination (averaged cos(ϕ))
Cell Density (cells mm-2)
0.065
0.06
0.055
0.05
0.045
0.04
0.035
0.03
0.025
0.02
0.015
0
100
200
300
400
500
600
700
800

d

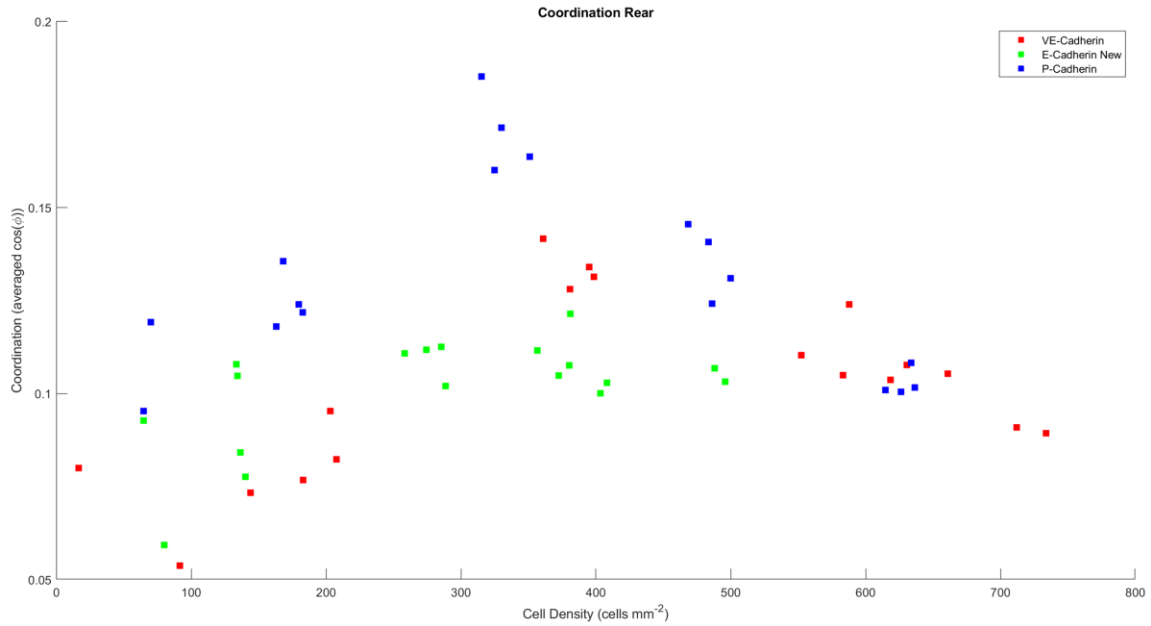
Coordination Rear
VE-Cadherin
E-Cadherin New
P-Cadherin
Coordination (averaged cos(ϕ))
Cell Density (cells mm-2)
0.2
0.15
0.1
0.05
0
100
200
300
400
500
600
700
800

e

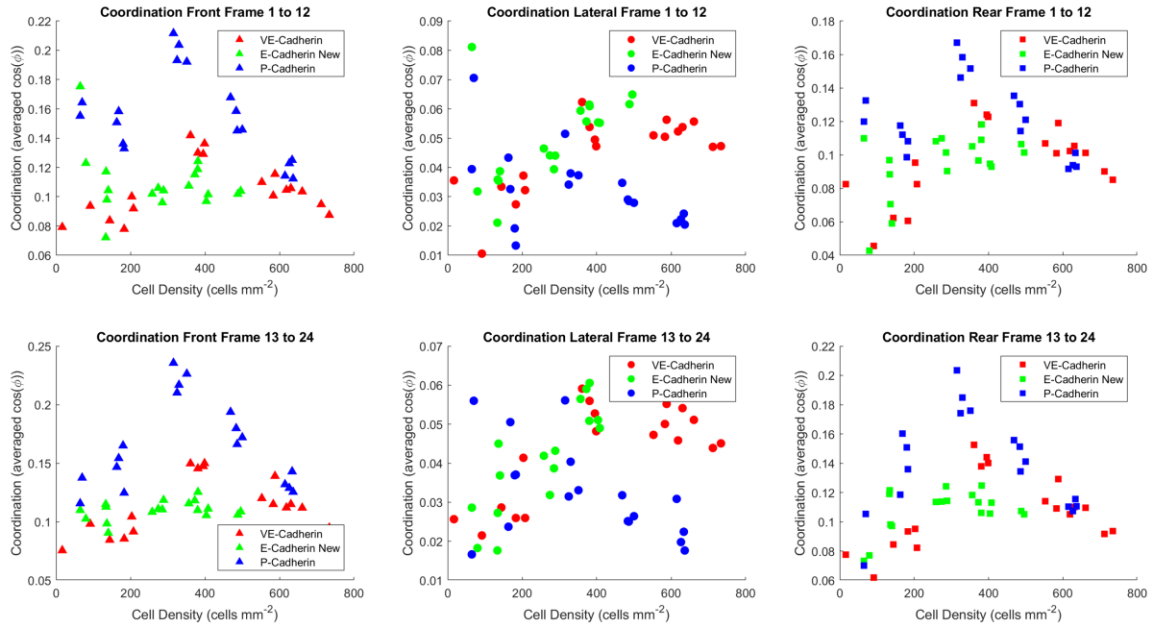

f

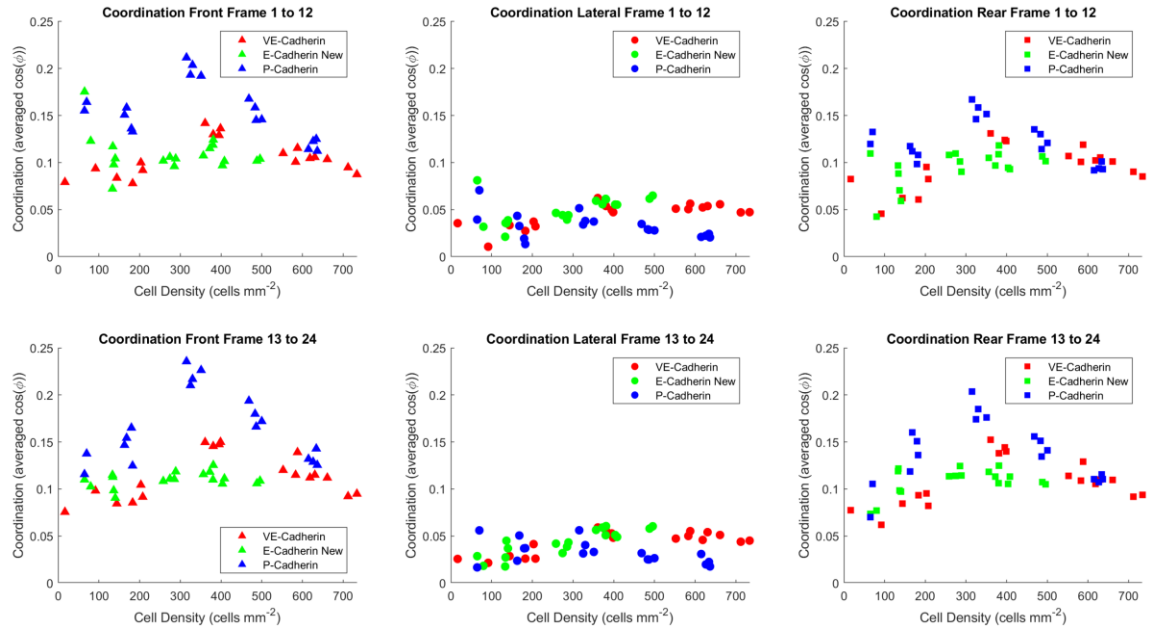

Figure 4 Coordination scores as a function of cell density in unperturbed monolayers. Each data point represents the averaged coordination values of all cells within an entire well and correspond to a single experiment. **(a)** The coordination values of each cadherin plated at different densities. Front **(b)**, lateral **(c)**, and rear **(d)** coordination values were calculated by taking neighbours present in a 60^{o} sector in the front, 120^{o} sector on the sides, and 60^{o} sector in the back of a cell, respectively. **(e)** The front (left), lateral (middle) and rear (right) coordinations split into the first half of microscopy (top) and second half of microscopy (bottom) and **(f)** controlling for the axis limits.

DISCUSSION, LIMITATIONS AND FUTURE DIRECTIONS

At lower cell densities (below 300 cells per mm^2), there is less cell-cell adhesion between cells resulting in less collective behaviour and therefore overall lower coordination as seen in E-cadherin, VE-cadherin, and P-cadherin. In this case, since the cells are not as close to one another, they may not be attached to leader cells and there may be random movement within the monolayer. At higher cell densities we observed more collective cell behaviour as seen in an increase in coordination with peak coordination occurring at 400 cells per mm^2 for all cell lines expressing different cadherin isoforms. While P-cadherin is important in the conservation of structural tissue integrity and shares around 67% of homology with E-cadherin (Vieira & Paredes, 2015), HUVECs expressing P-cadherin show very distinct differences in coordination within the front and lateral regions of cells compared to E-cadherin. From our results, we discovered that cells expressing E-, VE-, or P-cadherin usually peaked in coordination at around 400 cells per mm^2. At this peak coordination density, the front end of P-cadherin cells has coordination scores almost twice as high as E-cadherin cells and around 1.5 times higher than VE-cadherin cells. The rear coordination showed a similar trend to the front coordination results. For all cells, we observed that cells were primarily coordinated with cells at their front and rear as opposed to with cells at their sides as observed previously (Hayer et al., 2016). On the other hand, at peak coordination density, lateral coordination in P-cadherin is almost half the coordination of E-cadherin and VE-cadherin cells with E- and VE-cadherin cells following similar lateral coordination trends across all cell densities.

It has been shown that cadherin mechanosensing requires the formation of a stoichiometric complex involving cadherins and their adaptor proteins, β-catenin and α-catenin, which is able to bear force to transmit mechanical signals (Leckband, le Duc, Wang, & de Rooij, 2011). Adaptor proteins are indispensable when it comes to cell adhesion activity involving cadherins. For example, β-catenin is crucial for maintaining E-cadherin levels in the membrane through interaction with vinculin (Peng, Cuff, Lawton, & DeMali, 2010), but studies show that β-catenin in particular seems to be less as important as α-catenin since there is no significant loss in cadherin function when β-catenin is replaced by α-catenin-cadherin fusions (Imamura, Itoh, Maeno, Tsukita, & Nagafuchi, 1999). Studies show that α-catenin is an auto-inhibited protein that contains an inhibitory domain which blocks a vinculin-binding site adjacent to it (Yonemura, Wada, Watanabe, Nagafuchi, & Shibata, 2010). The further significance of α-catenin has been suggested in models which demonstrate its role in the cadherin-actomyosin complex where α-catenin auto-inhibition is relieved through increased mechanical stress (Leckband et al., 2011). The significance of tension stems from its involvement in leader-follower cell relationships and signalling across junctions. E-cadherin expressing cells have been shown to display three types of tensile bonds: catch bonds which strengthen when pulled such that bonds become longer-lived, slip bonds which when pulled become weaker and shorter-lived, and lastly ideal bonds which are insensitive to mechanical stress (Rakshit, Zhang, Manibog, Shafraz, & Sivasankar, 2012). Considering that P-cadherin expressing cells display higher front-rear coordination in comparison to E- and VE-cadherin expressing cells, this may suggest that P-cadherin has stronger binding interactions than E- or VE-cadherin. In addition, P-cadherin and E-cadherin show different responses to stress. One study showed that P-cadherin coated beads displayed oscillatory displacement patterns of constant amplitude when pulled on while E-cadherin coated beads showed displacements with a decrease in amplitude over time (Bazellières et al., 2015). Thus, since tension is crucial for α-catenin function and may be involved in different cadherin binding strengths, I would hypothesize that with respect to the intracellular domain, the presence or absence of α-catenin could be used to test for coordination differences in P-

cadherin and E- or VE-cadherin-expressing HUVEC. To do so, siRNA knockdown or knockout of α-catenin in HUVEC expressing different cadherin isoforms should be further investigated.

A limitation of this study involves the difference in cell sizes between P-cadherin and the E- and VE-cadherin expressing cells. Since larger cells may have a smaller surface area to volume ratio, they may have the disadvantage of a decreased rate of diffusion and transport of nutrients across their cell surface. Slower diffusion rates and surface area to volume ratio could affect the rate of signal transduction across the cell membrane as well as the speed of cell-cell communication and thus result in a slower response to signals for cell turning and detachment from the collectively migrating group, factors which could decrease the coordination. Since P-cadherin HUVECs were generally larger than VE-cadherin and E-cadherin cells which were relatively similar in size (data not shown), the slower response to cell turning could explain the reason for P-cadherin cells having much larger front and rear coordination of the three cell groups. Furthermore, since the major coupling mechanisms mediating collective migrations is between the rear of leader cells and front of follower cells rather than the sides (Hayer et al., 2016), having a smaller surface area to volume ratio could result in a weaker ability to polarize cells side by side and would result in weaker lateral coordination. This is consistent with the results as VE-cadherin and E-cadherin cells were generally of similar size and their lateral coordination scores were almost indistinguishable. Moreover, P-cadherin cells also had much higher speeds than E-cadherin cells which were in turn slightly faster than VE-cadherin cells. Since cell polarization can occur in small cells (immune cells) just as much as in large cells and polarization of cells migrating in sheets is independent of growth factor signaling (Vitorino, 2009), this would not explain the higher speeds of P-cadherin expressing cells nor the greater decrease in speeds at cell densities above 400 cells per mm^2 whereas the VE- and E-cadherin cells continued to move at relatively same speeds at this higher density compared to at lower cell densities. The speed of cells seems to play a role in determining coordination in P-cadherin cells since at the cell density of ~400 cells per mm^2 where peak coordination occurs, we also see the fastest cells. However, cell speed seems to have a smaller influence in E- and VE-cadherin cells since speeds stay relatively similar through all densities whereas coordination tends to peak at 400 cells per mm^2. Nevertheless, cell sizes should be controlled for to reduce the number of variables that could potentially affect coordination between cells.

Another limitation of this study involves the decreased growth rate of E-cadherin cells. These cells (new construct) grew at a much slower rate than P-cadherin and VE-cadherin cells possibly because of forced high expression in endothelial cells rather than their native epithelial cells. In support of this, we found that VE-cadherin HUVECs which endogenously express VE-cadherin seemed to grow at the fastest rate amongst the three cadherin cell lines when growing cells for experimentation. On the other hand, E-cadherin cells proliferated the slowest out of the three. Studies have shown that when E-cadherin is ectopically expressed in epithelial cells, cell growth tends to slow and can arrest in G1 phase (Stockinger, Eger, Wolf, Beug, & Foisner, 2001). While we are working in endothelial cells, we are nevertheless forcing E-cadherin expression and this may lead to the slowed growth in E-cadherin cells. Slower E-cadherin proliferation would affect cell density as after plating, cells were incubated at 37°C for close to 24 hours. Since HUVEC cells double between 24 – 36 hours, cell division would have had a chance to occur. The decreased growth rates of E-cadherin would be visible as a shift in cell density to the left towards lower densities compared to the VE- and P-cadherin cell lines and could explain why cell densities seemed to be uneven. Another limitation involves the analysis of data significance. While performing ANOVA, homogeneity of variance was assumed for the data sets and if this was violated, then Levene's Test or Welch's ANOVA should have been run instead. Furthermore, a further aspect of this study that should have been controlled for includes scientific objectivity

such as determining and designing the statistical tests to be conducted prior to the start of the experiment.

For further exploration other than siRNA knockdown or knockout of α-catenin, we could investigate collective cell behaviour when switching up cadherin intracellular domains. Since we have shown that P-cadherin is significantly different from both E-cadherin (new construct) and VE-cadherin at 0 – 250 cells per mm^2 and 250 – 500 cells per mm^2 for the front coordination and 250 – 500 cells per mm^2 for the lateral coordination, we could potentially switch up the intracellular domains of P-cadherin with either VE-cadherin or E-cadherin. Studies have shown that p120-catenin plays a role in cadherin stabilization and regulation of cadherin levels and also acts as a limiting factor and can cause endogenous cadherins to be degraded through competition for p120-catenin binding (Maeda et al., 2006). Further studies show that when both P-cadherin and E-cadherin are co-expressed in breast carcinomas, membrane staining for p120-catenin decreases and it becomes increasingly localized within the cytoplasm (Taniuchi et al., 2005). Thus, to perform the intracellular domain switch we could increase the amount of exogenous cadherin to flush out the endogenous cadherin as a potential solution but this does not always work as other factors may be involved as well. However, if E-cadherin is ultimately chosen, before testing with P-cadherin, we should analyze the E-cadherin (new) with immunofluorescence since the new E-cadherin construct (Fig. 3, 4) showed similar trends as the old E-cadherin cell line (Fig. 1) in single cell velocity and coordination. While the old E-cadherin cell line showed little VE-cadherin expression within junctional regions, we did not perform immunofluorescence analysis on the new E-cadherin cell line and should do so as a control and check for its VE-cadherin levels against the old E-cadherin immunofluorescence images.

Acknowledgements

We thank the Dankort, Moon, Brouhard and Vogel Lab for sharing their lab space, tissue culture room, and workstations. We thank Dr. Erika Wee of the Advanced BioImaging Facility for training in MetaXpress6 software and Microscopy. We are grateful for Grace Hu, Ivy Wang, and Katerina Zouboulakis for help with MATLAB and cell tracking analysis as well as their active participation in lab meetings to discuss the project.

I thank Arnold Hayer for his time, patience, insight and for the training in tissue culture, live-cell imaging, MATLAB analysis, and for allowing me to use his lab and resources to conduct this project.

References

Bazellières, E., Conte, V., Elosegui-Artola, A., Serra-Picamal, X., Bintanel-Morcillo, M., Roca-Cusachs, P., … Trepat, X. (2015). Control of cell-cell forces and collective cell dynamics by the intercellular adhesome. *Nature Cell Biology*, *17*(4), 409–420. https://doi.org/10.1038/ncb3135

Dilla, T., & Sacristan, J. (2006). Evaluación económica de Intervenciones Sanitarias. *Doyma*, 699–701. https://doi.org/10.1160/TH05

Engle, K. M.; Mei, T-S.; Wasa, M.; Yu, J.-Q. (2008). NIH Public Access. *Accounts of Chemical Research*, *45*(6), 788–802. https://doi.org/10.1038/jid.2014.371

Friedl, P., & Gilmour, D. (2009). Collective cell migration in morphogenesis, regeneration and cancer. *Nature Reviews Molecular Cell Biology*, *10*(7), 445–457. https://doi.org/10.1038/nrm2720

Friedl, P., Locker, J., Sahai, E., & Segall, J. E. (2012). Classifying collective cancer cell invasion. *Nature Cell Biology*, *14*(8), 777–783. https://doi.org/10.1038/ncb2548

Halbleib, J. M., & Nelson, W. J. (2006). Cadherins in development: Cell adhesion, sorting, and tissue morphogenesis. *Genes and Development*, *20*(23), 3199–3214. https://doi.org/10.1101/gad.1486806

Hayer, A., Shao, L., Chung, M., Joubert, L. M., Yang, H. W., Tsai, F. C., … Meyer, T. (2016). Engulfed cadherin fingers are polarized junctional structures between collectively migrating endothelial cells. *Nature Cell Biology*, *18*(12), 1311–1323. https://doi.org/10.1038/ncb3438

Imamura, Y., Itoh, M., Maeno, Y., Tsukita, S., & Nagafuchi, A. (1999). Functional domains of ??-catenin required for the strong state of cadherin-based cell adhesion. *Journal of Cell Biology*, *144*(6), 1311–1322. https://doi.org/10.1083/jcb.144.6.1311

Leckband, D. E., le Duc, Q., Wang, N., & de Rooij, J. (2011). Mechanotransduction at cadherin-mediated adhesions. *Current Opinion in Cell Biology*, *23*(5), 523–530. https://doi.org/10.1016/j.ceb.2011.08.003

Maeda, M., Johnson, E., Mandal, S. H., Lawson, K. R., Keim, S. A., Svoboda, R. A., … Johnson, K. R. (2006). Expression of inappropriate cadherins by epithelial tumor cells promotes endocytosis and degradation of E-cadherin via competition for p120ctn. *Oncogene*, *25*(33), 4595–4604. https://doi.org/10.1038/sj.onc.1209396

Marie, P. J., Haÿ, E., Modrowski, D., Revollo, L., Mbalaviele, G., & Civitelli, R. (2014). Cadherin-mediated cell-cell adhesion and signaling in the skeleton. *Calcified Tissue International*, *94*(1), 46–54. https://doi.org/10.1007/s00223-013-9733-7

Mayor, R., & Etienne-Manneville, S. (2016). The front and rear of collective cell migration. *Nature Reviews Molecular Cell Biology*, *17*(2), 97–109. https://doi.org/10.1038/nrm.2015.14

McCann, C. P., Kriebel, P. W., Parent, C. A., & Losert, W. (2010). Cell speed, persistence and

information transmission during signal relay and collective migration. *Journal of Cell Science*, *123*(10), 1724–1731. https://doi.org/10.1242/jcs.060137

Peng, X., Cuff, L. E., Lawton, C. D., & DeMali, K. A. (2010). Vinculin regulates cell-surface E-cadherin expression by binding to -catenin. *Journal of Cell Science*, *123*(4), 567–577. https://doi.org/10.1242/jcs.056432

Rakshit, S., Zhang, Y., Manibog, K., Shafraz, O., & Sivasankar, S. (2012). Ideal, catch, and slip bonds in cadherin adhesion. *Proceedings of the National Academy of Sciences*, *109*(46), 18815–18820. https://doi.org/10.1073/pnas.1208349109

Stockinger, A., Eger, A., Wolf, J., Beug, H., & Foisner, R. (2001). transcriptional activity, *154*(6), 1185–1196. https://doi.org/10.1083/jcb.200104036

Taniuchi, K., Nakagawa, H., Hosokawa, M., Nakamura, T., Eguchi, H., Ohigashi, H., … Nakamura, Y. (2005). Overexpressed P-cadherin/CDH3 promotes motility of pancreatic cancer cells by interacting with p120ctn and activating Rho-family GTPases. *Cancer Research*, *65*(8), 3092–3099. https://doi.org/10.1063/1.1142502

Vieira, A. F., & Paredes, J. (2015). P-cadherin and the journey to cancer metastasis. *Molecular Cancer*, 1–12. https://doi.org/10.1186/s12943-015-0448-4

Vitorino, P. M. (2009). Modular Control of Endothelial Sheet Cohesion and Collective Cell Migration. *Stanford University Thesis*, *1*, 3268–3281. https://doi.org/10.1101/gad.1725808.tracheal

Xiao, K., Oas, R. G., Chiasson, C. M., & Kowalczyk, A. P. (2007). Role of p120-catenin in cadherin trafficking. *Biochimica et Biophysica Acta - Molecular Cell Research*, *1773*(1), 8–16. https://doi.org/10.1016/j.bbamcr.2006.07.005

Yonemura, S., Wada, Y., Watanabe, T., Nagafuchi, A., & Shibata, M. (2010). α-Catenin as a tension transducer that induces adherens junction development. *Nature Cell Biology*, *12*(6), 533–542. https://doi.org/10.1038/ncb2055

Other References (Statistical Tests)

Balanced and unbalanced designs in ANOVA models. Retrieved from http://support.minitab.com/en-us/minitab/17/topic-library/modeling statistics/anova/anova-models/balanced-and-unbalanced-designs/

Barros, F. (2013). ANOVA and Tukey's Test on R. Retrieved from http://www.r-bloggers.com/anova-and-tukeys-test-on-r/

Chan, P. (2011, January 22). Statistics with R: One Way ANOVA example 1 of 2 [Video file]. Video posted to https://www.youtube.com/watch?v=T0Lmyz6EscY&feature=youtu.be

Confidence Intervals. Retrieved from http://www.statsdirect.com/help/content/basics/confidence_interval.htm

Kabacoff, R. (2011). *R in Action: Data Analysis and Graphics with R*. Shelter Island, NY: Manning Publications Company.

Kephart, C. (2011, July 26). Loading Data into R Software [Video file]. Video posted to https://www.youtube.com/watch?v=VLtazaiYo-c

Lund, A. & Lund, M. (2013). One Way ANOVA. Retrieved from https://statistics.laerd.com/statistical-guides/one-way-anova-statistical-guide.php

Nayak, B. K., & Hazra, A. (2011). How to choose the right statistical test?. *Indian journal of ophthalmology*, *59*(2), 85-6.

One Way Analysis of Variance. Retrieved from http://www.statsdirect.com/help/Default.htm#analysis_of_variance/one_way.htm

P Values. Retrieved from http://www.statsdirect.com/help/default.htm#basics/p_values.htm

Shuttleworth, M. (2008). Significance Test. Retrieved from https://explorable.com/significance-test

RStudio [Computer Software]. (2015). Available from https://www.rstudio.com/

Simon, S. (2005). When the F test is significant, but Tukey is not. Retrieved from http://pmean.com/05/TukeyTest.html

What are Type I and Type II Errors?. Retrieved from http://support.minitab.com/en-us/minitab/17/topic-library/basic-statistics-and-graphs/hypothesis-tests/basics/type-i-and-type-ii-error/

Appendix: ANOVA and post-hoc test data values for comparison of VE-, E-, and P-cadherin

Appendix 1: Coordination 0 – 250 cells per mm^2 density

ANOVA shows there is a significance

```
##             Df   Sum Sq   Mean Sq F value Pr(>F)
## Cadherin     2 0.001216 0.0006083   5.534 0.0158 *
## Residuals   15 0.001649 0.0001099
## ---
## Signif. codes:  0 '***' 0.001 '**' 0.01 '*' 0.05 '.' 0.1 ' ' 1
```

Tukey HSD shows significance between P-VE

```
             diff          lwr         upr     p adj
E-VE 0.009934915 -0.005787788 0.02565762 0.2595973
P-VE 0.020136740  0.004414037 0.03585944 0.0120367
P-E  0.010201825 -0.005520878 0.02592453 0.2428661
```

Appendix 2: Coordination 250 – 500 cells per mm^2 density

ANOVA shows no significance

```
            Df    Sum Sq   Mean Sq F value Pr(>F)
Cadherin     2 0.0003649 1.824e-04   2.402  0.115
Residuals   21 0.0015946 7.593e-05
```

Appendix 3: Front Coordination 0 – 250 cells per mm^2 density

ANOVA shows high significance

```
##             Df   Sum Sq  Mean Sq F value   Pr(>F)
## Cadherin     2 0.009765 0.004882   27.01 1.07e-05 ***
## Residuals   15 0.002712 0.000181
## ---
## Signif. codes:  0 '***' 0.001 '**' 0.01 '*' 0.05 '.' 0.1 ' ' 1
```

Tukey HSD: significance in E-VE, P-VE, P-E

```
## $Cadherin
##             diff          lwr        upr     p adj
## E-VE 0.02114788 0.0009839401 0.04131183 0.0392788
## P-VE 0.05646276 0.0362988170 0.07662670 0.0000077
## P-E  0.03531488 0.0151509338 0.05547882 0.0010518
```

Appendix 4: Front Coordination 250 – 500 cells per mm^2 density

ANOVA shows high significance

```
##             Df   Sum Sq Mean Sq F value   Pr(>F)
## Cadherin     2 0.030105 0.01505   60.19 2.02e-09 ***
## Residuals   21 0.005252 0.00025
## ---
## Signif. codes:  0 '***' 0.001 '**' 0.01 '*' 0.05 '.' 0.1 ' ' 1
```

Games-Howell Test: significance in all three comparisons

```
## ### Post hoc test: games-howell
##
##       diff ci.lo ci.hi     t   df     p
## P-E   0.08  0.05  0.11  8.45 7.63 <.001
## VE-E  0.03  0.02  0.04 11.52 9.35 <.001
## VE-P -0.05 -0.07 -0.02  5.06 7.62  .003
```

Appendix 5: Lateral Coordination 0 – 250 cells per mm^2 density

ANOVA shows no significance

```
##             Df    Sum Sq   Mean Sq F value Pr(>F)
## Cadherin     2 0.0002032 0.0001016   0.724  0.501
## Residuals   15 0.0021044 0.0001403
```

Appendix 6: Lateral Coordination 250 – 500 cells per mm^2 density

ANOVA shows significance

```
##             Df   Sum Sq   Mean Sq F value   Pr(>F)
## Cadherin     2 0.001746 0.0008732   12.33 0.000287 ***
## Residuals   21 0.001487 0.0000708
## ---
## Signif. codes:  0 '***' 0.001 '**' 0.01 '*' 0.05 '.' 0.1 ' ' 1
```

Games-Howell Test shows significance between P-E and VE-P but no significance with VE-E

```
## ### Post hoc test: games-howell
##
##       diff ci.lo ci.hi    t    df    p
## P-E  -0.02 -0.03 -0.01 4.37 14.77 .002
## VE-E  0.00 -0.01  0.01 0.40  8.30 .918
## VE-P  0.02  0.01  0.03 4.53  9.19 .003
```

Supplementary Figures

Figure S1. Single cell velocity of E-cadherin (old) and VE-cadherin as a function of cell density were calculated similar to Figure 1a. In this case, only cells present within the field of view of the microscope during the full 2 hour imaging were used to calculate velocity and any cells that left or entered the FOV were excluded from calculation.

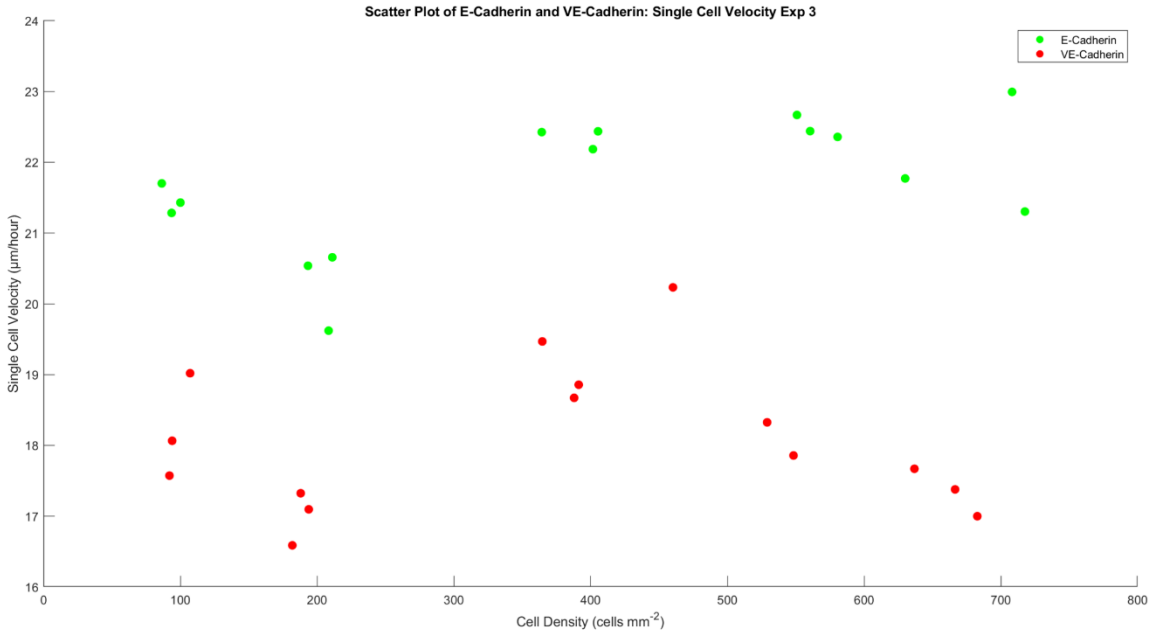

Figure S2 Single cell velocity analysis of fixed VE-cadherin, E-cadherin(new) and P-cadherin cells in an unperturbed monolayer with data calculated only from cells present in the FOV during the entire microscopy period. Cells leaving or entering the FOV at different time points during microscopy were exluded from the calculation. **(a)** The overal single cell velocity averaged over 2 hours and **(b)** single cell velocity split between the first hour of microscopy (left) and the second hour of microscopy (right) as a function of cell density.

a

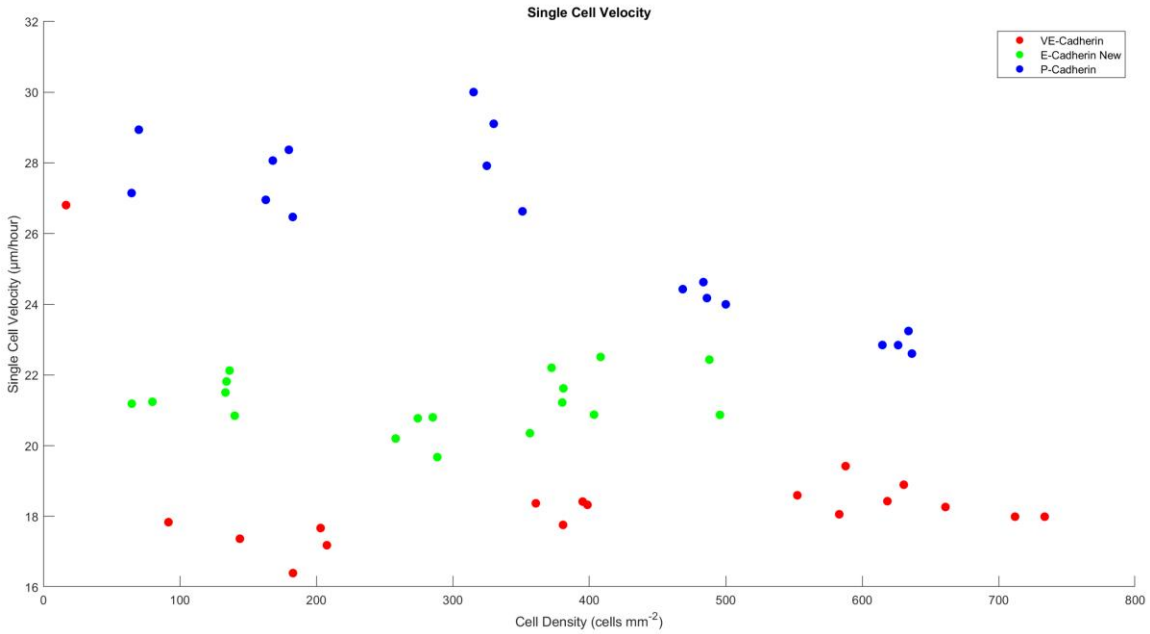

b

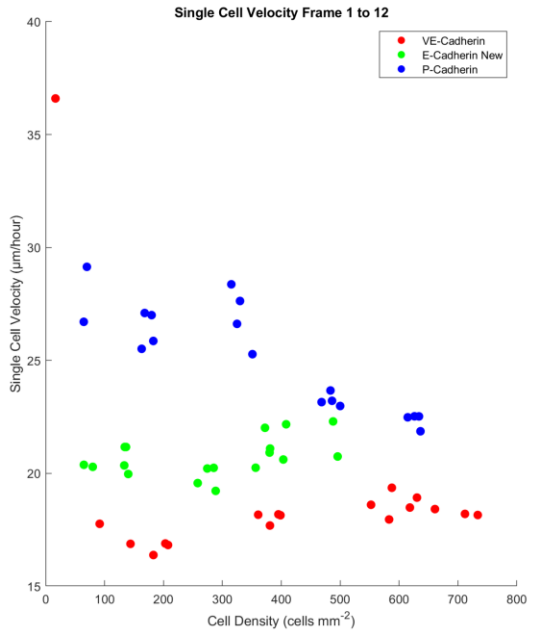

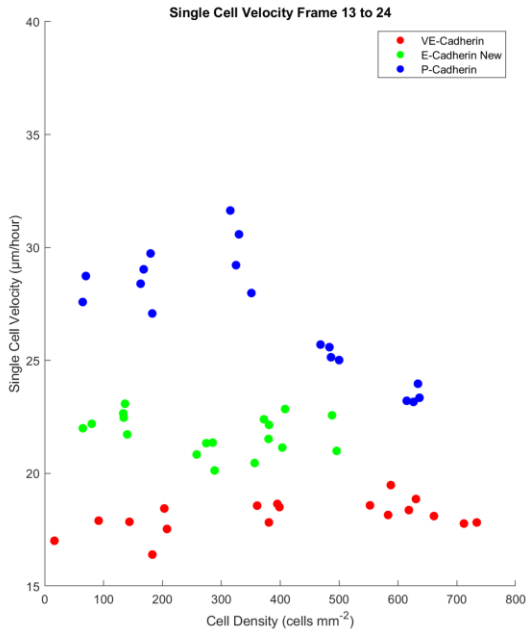

Figure S3 The coordination of VE-, E- (new), and P-cadherin cells split between the first hour of microscopy (left) and the second hour of microscopy (right) as a function of cell density.